Aalto University

Aaltodoc
OPEN ACCESS

This is an electronic reprint of the original article.
This reprint may differ from the original in pagination and typographic detail.

Author(s): Hauru, Lauri; Hummel, Michael; King, Alistair; Kilpeläinen, Ilkka; Sixta, Herbert

Title: Role of solvent parameters in the regeneration of cellulose from ionic liquid solutions

Year: 2012

Version: Final published version

Please cite the original version:

Hauru, Lauri; Hummel, Michael; King, Alistair; Kilpeläinen, Ilkka; Sixta, Herbert. 2012. Role of solvent parameters in the regeneration of cellulose from ionic liquid solutions. American Chemical Society, Biomacromolecules, volume 13, issue 9, pages 2896-2905. ISSN 1525-7797. DOI: 10.1021/bm300912y

Rights: © 2012 American Chemical Society. Reprinted with permission.

This publication is included in the electronic version of the article dissertation:
Hauru, Lauri K.J. Lignocellulose solutions in ionic liquids.
Aalto University publication series DOCTORAL DISSERTATIONS, 87/2017.

All material supplied via Aaltodoc is protected by copyright and other intellectual property rights, and duplication or sale of all or part of any of the repository collections is not permitted, except that material may be duplicated by you for your research use or educational purposes in electronic or print form. You must obtain permission for any other use. Electronic or print copies may not be offered, whether for sale or otherwise to anyone who is not an authorised user.

Article

pubs.acs.org/Biomac

Role of Solvent Parameters in the Regeneration of Cellulose from Ionic Liquid Solutions

Lauri K. J. Hauru,[†] Michael Hummel,[†] Alistair W. T. King,[‡] Ilkka Kilpeläinen,[‡] and Herbert Sixta*[,†]

[†]Department of Forest Products Technology, Aalto University, P.O. Box 16300, FI-00076 Aalto, Finland

[‡]Department of Chemistry, University of Helsinki, P.O. Box 55 (A. I. Virtasen aukio 1), FI-00014 Helsinki, Finland

Supporting Information

ABSTRACT: The ionic liquids 1-ethyl-3-methylimidazolium acetate [emim]OAc, *N,N,N,N*-tetramethylguanidium propionate [TMGH]$EtCO_2$, and *N,N,N,N*-tetramethylguanidium acetate [TMGH]OAc, and the traditional cellulose solvent *N*-methylmorpholine *N*-oxide NMMO were characterized for their Kamlet–Taft (KT) values at several water contents and temperatures. For the ionic liquids and NMMO, thresholds of regeneration of cellulose solutions by water were determined using nephelometry and rheometry. Regeneration from wet IL was found to be asymmetric compared to dissolution into wet IL. KT parameters were found to remain almost constant at temperatures, between 20–100 °C, even at different water contents. Among the KT parameters, the β value was found to change most drastically, with an almost linear decrease upon addition of water. The ability of the mixtures to dissolve cellulose was best explained by the difference $\beta-\alpha$ (net basicity), rather than β alone. Regeneration of cellulose starts at thresholds values of approximately $\beta < 0.8$ ($\beta-\alpha < 0.35$) and displayed four phases.

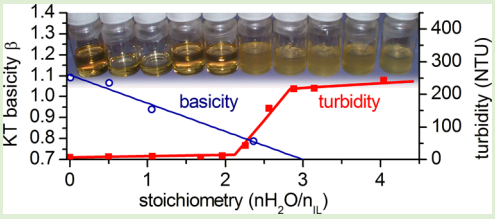

INTRODUCTION

The ability of ionic liquids (ILs) to dissolve cellulose and the precipitation of the cellulose, upon addition of water or other antisolvents, has been subject of much recent interest. Because cellulose cannot be melt-processed, processing of cellulose requires either derivatization into cellulose xanthate (viscose) or dissolution into a direct solvent.[1] Currently, the only commercialized direct solvent process uses the monohydrate of *N*-methylmorpholine *N*-oxide (NMMO),[2,3] which is problematic because the cyclic ether bears a redox-active moiety and is prone to dangerous runaway decomposition.[4] ILs are generally thermally stable and thus less hazardous, suitable ILs could potentially replace NMMO·H_2O as a direct solvent. However, the behavior of cellulose-IL solutions needs to be properly characterized prior to establishing a process in larger scale.

Cellulose is insoluble in water at moderate temperatures because the intra- and intermolecular H-bonds, that give rise to its rigid three-dimensional sheet-like structure, are stronger than bonds to water.[5] Nevertheless, cellulose oligomers (DP < 6) can be dissolved in water, indicating that the thermodynamics of solvation are roughly favorable for aqueous solutions.[6] Decrystallized higher DP cellulose (DP 1200) could also be dissolved in cold aqueous NaOH.[7] Other than aqueous solvents, solutions such as the molten salt-based alkylpyridinium chlorides,[8] LiCl/DMAc (lithium chloride/*N,N*-dimethylacetamide),[9,10] NMMO·H_2O[2], and ILs (low temperature molten salts), such as 1-butyl-3-methylimidazolium chloride,[11] have demonstrated effective dissolution of cellulose. Spange et al.[12] proceeded to demonstrate that the H-bond basicity of LiCl/DMAc, a common feature of all the aforementioned solvents, is correlated to the breakage of H-bonds between cellulose chains, resulting in the dissolution of cellulose. The authors characterized the solvents in terms of their Kamlet–Taft (KT) parameters[13] α (H-bond acidity), β (H-bond basicity), and π^* (dipolarity/polarizability ratio); to determine α, the $E_T(30)$ polarity parameter (transition energy of Reichardt's dye in kcal/mol)[14,15] is also required. Similar parametrization methodologies have been used for modern day ILs and room temperature ionic liquids (RTILs), concerning the solubility of cellulose[16−20] or swelling of wood.[21] As yet, further correlations with parameters other than H-bond basicity have not been observed for ionic liquids. In the case of molecular solvents, correlation of the swelling percentage with solvent parameters requires multiple parameter regression. Correlations of vapor sorption are observed with molar volume, with the ability to interact with cellulose hydroxyls and with dielectric constants, although the latter holds only in series of similar compounds.[22] Many molecular solvents are good swelling agents for cellulose, but only a few, such as ethanolamine, dimethyl sulfoxide, formamide, and dimethylformamide, are comparable or better than water.[22] No correlation is evident with density, viscosity, surface tension, dielectric constant, dipole moment, cohesive energy density, or $E_T(30)$ value. However, the polar δ_P, hydrogen bonding δ_H, and molar volume components of cohesive energy density (Hildebrand parameter) have been correlated with swelling.[23] According to El Seoud et al.,[24] the best fits are with π^* for native and

Received: June 14, 2012
Revised: August 1, 2012
Published: August 7, 2012

 © 2012 American Chemical Society

microcrystalline cellulose, and with V_s (solvent molar volume) for mercerized cellulose.

These correlations indicate a dependency on both the enthalpic and entropic contributions to the dissolution process although to date, the link between these contributions and various parameters still needs clarification. Computational studies have attributed solubility of high DP cellulose to favorable enthalpies of solvation,[25] which is linked to solvent basicity. For example, the basic anion acetate can form strong H-bonds that enable cellulose dissolution. The strength of the intramolecular H-bonds that keep cellulose rigid are 25 kJ mol^{-1},[22] but the strength of the water-cellulose H-bond is only 17 or 21 kJ mol^{-1} with cellulose OH as an acceptor or as a donor, respectively.[25] In contrast, the acetate anion can form a bond of 59 kJ mol^{-1}.[25] In comparison, the van der Waals bond strength is 0.15 kJ mol^{-1} and the OH covalent bond strength is 460 kJ mol^{-1}.[22] Addition of water, rehydrating the anion, typically causes a drop in β, which correlates with precipitation of cellulose from solution. Whether β is the only solvation parameter relevant that remains to be shown. An IL-based solvent prediction strategy that takes into account the entropic contribution to dissolution has been best demonstrated by Kahlen et al.[26] Despite the ability of this model to confirm known cellulose-dissolving ILs, it overestimates the combinatorial entropy term of the activity coefficient, leading to excessively large differences in entropy of mixing between ILs and, thus, overestimated differences of cellulose solubility. Correlation of the residual part of the activity coefficient, which subsumes all specific energetic solvent−solute contributions, is successful within a series of different imidazolium halide ILs, but accurate determination of other parameters for better generality presents considerable theoretical and experimental challenges. However, an interesting prediction is that ILs with nonbasic anions, such as hexafluorophosphate, can dissolve cellulose if the cation interacts strongly with cellulose. Particularly, guanidinium derivatives, and generally, the combinations of large bulky cations with nondiffuse anions, such as hexamethylguanidinium acetate, should be highly suitable for cellulose dissolution.

Recently, King et al. published a class of distillable ILs based on the *N,N,N,N*-tetramethylguanidium cation ([TMGH]$^+$).[27] Their cellulose solvation capabilities are similar to that of imidazolium-based ILs when dry, but, in addition, they can be recycled via distillation. In the current study, we proceed to characterize tetramethylguanidium acetate and propionate ([TMGH]OAc and [TMGH]EtCOO, Figure 1a and b) in terms of their Kamlet−Taft parameters as a function of temperature and water content. This served as a starting point to correlate the change of respective KT values with the ILs' capability to dissolve cellulose. The well known cellulose solvent systems, 1-ethyl-3-methylimidazolium acetate ([emim]-OAc, Figure 1c),[28] NMMO·H_2O (Figure 1d), and LiCl/DMAc, were selected for comparison. The thresholds of cellulose solubility were determined via quantifying the increase of turbidity upon regeneration, using a method described by Mazza et al.[29] This method enables the detection of not only the start of regeneration, but also the end point, where the solution turns into an aqueous suspension. Furthermore, intermediate gel formation was followed with rheological measurements. Thus, this study is an attempt to develop further insight, from our Kamlet−Taft measurements and numerous literature values, into the thermodynamic requirements for dissolution and regeneration of cellulose as two separate and nonidentical processes.

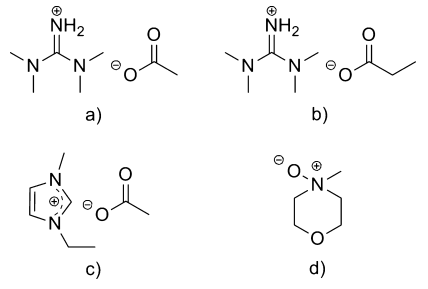

Figure 1. Structural formula of (a) *N,N,N,N*-tetramethylguanidium acetate [TMGH]OAc, (b) *N,N,N,N*-tetramethylguanidium propionate [TMGH]$EtCO_2$, (c) 1-ethyl-3-methylimidazolium acetate [emim]-OAc, and (d) *N*-methylmorpholine *N*-oxide NMMO.

MATERIALS AND METHODS

Materials. 1-Ethyl-3-methylimidazolium acetate ([emim]OAc, 98%) was purchased from Iolitec GmbH, Germany. Acetic acid (99%), propionic acid (99%), and the dyes, Reichardt's dye (RD), 4-nitroaniline (NA), and *N,N*-diethyl-4-nitroaniline (DENA), were purchased from Sigma-Aldrich, Germany. Tetramethylguanidine (TMG, 99%) was from ABCR GmbH, Germany. Prehydrolysis-kraft dissolving pulp from *Eucalyptus urograndis*, with 93% cellulose I, M_w = 291 kg/mol, M_n = 62 kg/mol, and PDI = 3.5 (Bahia Specialty Cellulose, Brazil), was used. The sheets were cut to a powder in a Wiley mill with 1 mm sieve and then oven-dried at 105 °C to constant weight.

Tetramethylguanidium ([TMGH]$^+$) ILs were synthesized by carefully adding the respective acid to neat TMG. A dropping funnel was used when preparing large amounts, such that the temperature remained below 80 °C, as measured with a noncontact thermometer. This was followed by stirring at 80 °C for 1/2 h. Smaller amounts (ca. 10 mL) for KT parametrization could be mixed directly. A very small excess of TMG below 10^{-3} in stoichiometric units was used to avoid Brønsted acidity of the solvent.

Anhydrous NMMO (97% from SigmaAldrich) was hydrated in acetone with 1.21 equiv of water (5 w/w % water in acetone) and recrystallized to give the monohydrate (mp 75−77 °C, 13 w/w % H_2O).[30]

LiCl/DMAc was prepared by dissolving 6 w/w % anhydrous lithium chloride into dimethylacetamide at 90 °C.

Kamlet−Taft Parameters. The Kamlet−Taft parameters were determined from the absorption peaks of the three dyes, Reichardt's dye (RD, range 518−585 nm), *N,N*-diethyl-4-nitro-aniline (DENA, 402−414 nm), and 4-nitroaniline (NA, 406−398 nm). The dyes were weighed as is and mixed with the ILs to a peak absorbance of 0.2−2.5 AU (i.e., concentrations were RD 1.1, DENA 0.24, and NA 0.27 mmol/g). A Varian UV−vis spectrometer equipped with a thermostat (precision ±0.1 °C) was used. Deionized water was measured for background subtraction. Spectra were collected at a resolution of 1 nm and 10−30 nm of absorbance data around the peak was fitted with a Gaussian function in order to precisely locate the maxima (ν_{max}). The result was a resolution exceeding that of the instrument (1 nm).

From the collected peak data, a linear least-squares fit against temperature was done for an absorption maxima at 20−100 °C (typically $R^2 > 0.998$ for all dyes, standard deviation 0.05−0.09 nm). From these functions, ν_{max}(T), E_T(30), π^*, and α and β parameters were calculated as per literature (see Supporting Information, eqs S1−5).[16] The resulting uncertainty from ν_{max}(T) was ±0.008, ±0.001, ±0.001, and ±0.003 for E_T(30), π^*, α, and β, respectively, which is below the influence of other sources of error.

In [TMGH]OAc with 40 w/w % water, the Reichardt's dye peak was reduced to a weakly absorbing shoulder (A = 0.0002−0.003 above background). The resulting values of E_T(30) = 53.1 and α = 0.551 are inconsistent with other data. Possible reasons are protonation of the

dx.doi.org/10.1021/bm300912y | *Biomacromolecules* 2012, 13, 2896−2905

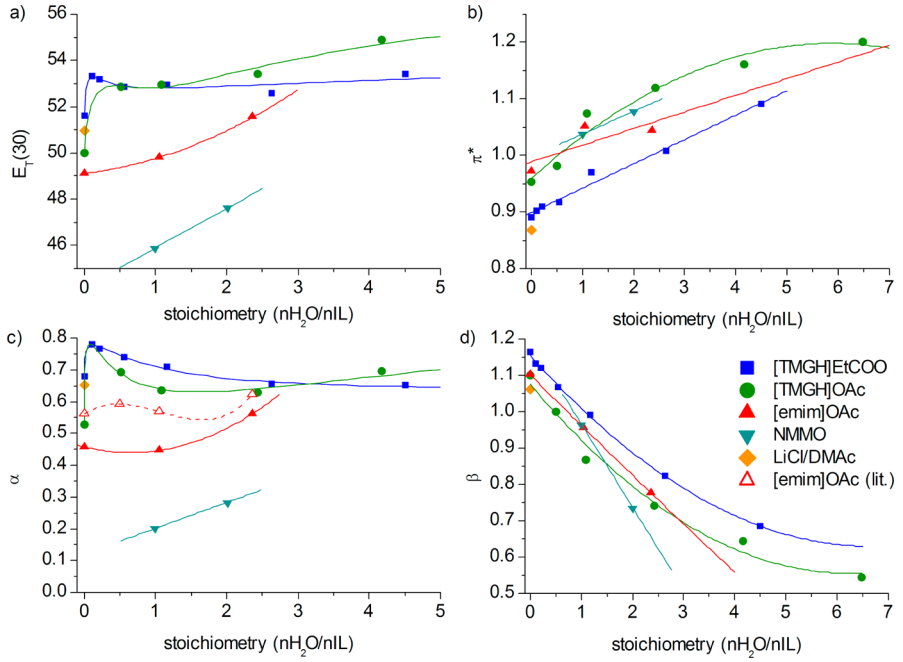

Figure 2. KT values (a) $E_T(30)$ polarity parameter, (b) π^* dipolarity/polarizability ratio, (c) α H-bond acidity, and (d) β H-bond basicity across water contents at 80 °C vs stoichiometry of water in the solution; LiCl/DMAc was measured only water-free; for comparison, α values by Doherty et al.[16] are included.

dye, preferential solvation by hydrophobic components (cf. mixtures of DMF with solvents[31,32]) or clustering of the dye, leading to polarity and acidity being underestimated.

IL–water mixtures were prepared gravimetrically (precision ±0.2% in absolute terms).

Dissolution and Regeneration. Clear 1 w/w % solutions in ILs could be produced simply by mixing oven-dried pulp with the IL at 80 °C. A 1 w/w % solution of pulp in NMMO was prepared by suspending the pulp in a 50 w/w % water–NMMO mixture, followed by evaporation of water under concomitant stirring to give a solution with 14.43 w/w % water (1.1 equiv, checked by KF). Similarly, a 9 w/w % solution of pulp was made by evaporation of water from a mixture of 50 g pulp, 443.2 g of water, and 500 g [emim]OAc, to a final water content of 9.7 w/w %. A vertical kneader system (b+b Gerätetechnik, Germany) described earlier[33] was used to knead the mix at 90 rpm and 80 °C and to gradually evaporate the water by means of a diaphragm vacuum pump (11 mbar max). This procedure is necessary because of the high viscosity of the final solution.

Cellulose solubility in [TMGH]OAc was tested using microcrystalline cellulose (MCC) as model substance. A total of 5 w/w % MCC were added to various [TMGH]OAc–water mixtures (0, 2, 4, 6, 8, and 10 w/w % water) and the resulting IL–water–cellulose mixtures were stirred overnight at 80 °C. The samples were cooled and turbidity estimated visually (see Supporting Information, Figure S1). Only the anhydrous sample was clear, but all wet samples remained turbid.

Regeneration experiments were done starting with a water-free 1 w/w % solution of pulp in IL. Water was added, the mix was sampled, and then topped up to give the next target water content. This was done no more than 4 times before starting with fresh water-free solution to minimize the risk of error accumulation. Homogenization was performed with an Ultra-Turrax high-shear mixer, air bubbles were removed by centrifugation (10000*g*, 10 min, 25 °C) and the samples were manually mixed to obtain a consistent mix. Mixtures exhibiting phase separation were remixed manually to obtain representative samples suitable for nephelometry. For the partially regenerated and gelatinous stages, the samples were processed below the sol–gel transition point, although in some cases temperatures could not be controlled precisely due to local overheating resulting from the high-shear mixing.

Nephelometry. Onset of precipitation was observed by nephelometry at 25 °C according to a published method, with modifications.[29] An Analite Model 156 (MacVan Instruments, Australia) backscatter nephelometer was modified such that the light shield was replaced with a black polyethylene cuvette of identical dimensions. The nephelometer was zeroed against water, except for the experiment with 9 w/w % pulp load and with NMMO·H_2O as the solvent, respectively, where the background turbidity was subtracted from the results. Thus, turbidity is expressed in terms of arbitrary units and cannot be compared between different solvent systems.

Rheology. Shear rheology of all solutions was measured on an Anton Paar MCR 300 rheometer with a plate and plate geometry. The viscoelastic domain was determined by performing a dynamic strain sweep test and a strain between 1 and 5%, which fell well within the linear viscoelastic regime, was chosen for the frequency sweep measurements. Due to the relatively high initial moisture content of the samples no significant additional water uptake from the laboratory atmosphere at the plate edges was observed within the required testing time. Thus, it was not necessary to seal the edges with paraffin oil as previously suggested.[34,35] Each sample was subjected to a dynamic frequency sweep at 25 °C over an angular velocity range of 0.1–100 s^{-1}. In addition, the [TMGH]OAc mixtures were heated stepwise in the range of 20–100 °C (2 °C step) with an angular frequency of 0.428 s^{-1} and strain of 1% to determine the influence of the temperature on the rheological key parameters (complex viscosity η^*, storage modulus G', and loss modulus G'').

RESULTS

Kamlet–Taft Parameters. The values were measured in the range of 20–100 °C, with the exception of NMMO hydrates, since NMMO·H_2O solidified below 50 °C and NMMO·$2H_2O$ below 30 °C (see Supporting Information, Tables S1 and S2 and Figure S2). Even though the melting points of [TMGH]$EtCO_2$ and [TMGH]OAc are 62 and 95 °C, respectively,[27] they supercooled easily and remained liquid for hours and even days when mixed with water. Hydrolysis of the IL or breakdown of the KT dyes was not observed. Temperature affected the KT parameters of all solvents and

dx.doi.org/10.1021/bm300912y | *Biomacromolecules* 2012, 13, 2896–2905

dyes in a linear manner. Only small deviations (0.02 units in terms of $E_T(30)$ and 0.001 in α) in the Reichardt's dye wavelength in NMMO·H_2O were found, which is connected to the complex phase transitions known for NMMO hydrates.[36]

The effect of temperature on KT values was small across substances and water contents. Reichardt's dye was the most thermochromic, but the resulting changes were minor, a 1.2−2.7 unit change in $E_T(30)$. Thus, only the RD-dependent KT values, π^* and α, changed significantly with temperature: π^* showed the most significant change, a consistent 0.15 decrease over the range of 20−100 °C for ILs, followed by a 0.05 unit decrease in α. β changed only about 0.02 units on average for the different ILs. The exception was LiCl/DMAc with a change $\Delta\beta = -0.120$ between 20−100 °C (see Supporting Information, Figure S2). The β value of dry [TMGH]OAc was indistinguishable from [emim]OAc across all temperatures (β = 1.09−1.10, see Supporting Information, Figure S2), but its acidity was slightly higher (α = 0.527 vs α = 0.458, Figure 2c).

[TMGH]$EtCO_2$ was slightly more basic (β = 1.164) and significantly more acidic (α = 0.678) than [TMGH]OAc (see leftmost points in Figure 2c and d); this increase in α follows from the higher $E_T(30)$ value and lower π^* value (see Supporting Information, eq S4). NMMO·H_2O, herein measured for the first time, was less basic than the pure ILs (β = 0.966) and of much lower acidity (α = 0.202, cf. acetonitrile[37]). For 6 w/w % LiCl/DMAc, the measured β = 1.140 disagrees with the very high value β = 1.95 measured by Spange et al. with a different set of dyes,[12] but the value is still consistent with other cellulose solvents.

The KT parameters were also assessed as a function of their water content. It has to be noted that this is not totally unambiguous. Previous studies have shown that the solvatochromic response of solvent mixtures can be misleading due to preferential interactions of the dye with one of the solvents or formation of microheterogeneities in the bulk phase, i.e. solvent cluster formation.[38] In a complex anion−cation−water system, this is rather likely to occur. However, we proceed presenting our results herein as the KT parameter could be reasonably correlated with the regeneration of cellulose (see Discussion).

Upon addition of water, β was found to decrease in an almost linear fashion for the [TMGH] ILs. The approximate slope was the same for different ILs (see Figure 2d). For [emim]OAc, the measured β agreed very well with literature.[16] NMMO hydrates were also in a similar range, but the β values were more sensitive to water, reflecting the high enthalpy of hydration of NMMO.

For the [TMGH] ILs, at the water concentrations above the initial rise, the α values leveled off and remained roughly constant over the increasing water stoichiometries. This is not unexpected as the aqueous pK_a of TMG is 13.6 at 25 °C.[39] NMMO hydrates revealed a very low acidity: the monohydrate afforded α = 0.202 and the dihydrate α = 0.284, due to the lack of any acidic position such as the C^2−H position in $[emim]^+$ or the protonated guanidinium N^2−H position in $[TMGH]^+$. Concerning dry [emim]OAc (α = 0.458), there was some minor disagreement between our data and different publications (α = 0.40[40] or 0.56[16]), best attributed to variable impurities originating from different synthesis methods.

The π^* values were also high for all liquids (π^* = 0.9−1.2) and increase on addition of water (Figure 2b). The 7% difference between [TMGH]$EtCO_2$ and [TMGH]OAc is best explained by the smaller size of the latter molecule. Furthermore, the addition of an extra methylene lowers dipolarity and increases polarizability, thus lowering the dipolarity/polarizability ratio. An increased dipolarity should promote cellulose solubility. Hence, the variations of π^* values in the ranges observed in this study do not seem to be relevant for cellulose solubility. However, for [TMGH] ILs, there is a limit to cellulose solubility as carboxylate chain length increases.[17]

$E_T(30)$ values did not change significantly across those water content ranges where regeneration occurred and moreover, NMMO had a consistently lower $E_T(30)$ value than the other solvents.

Regeneration and Nephelometry. The nephelometry plot showed three distinct sections: constant low turbidity, followed by a steep increase and, finally, a level-off phase (Figure 3). Thus, the regeneration process was divided into 3

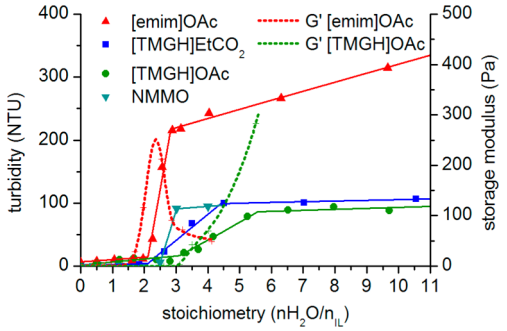

Figure 3. Regeneration of 1 w/w % cellulose solutions as a function of IL/H_2O stoichiometry, shown with turbidity and with the rheological storage modulus (G') of the 1 w/w % [emim]OAc and [TMGH]OAc solutions (measurements were performed at 25 °C).

parts where cellulose was dissolved (solution state), regenerating (transition state) and regenerated (suspension state), and each set of measurement points fitted with a linear function. The intersections were then defined as start and end point of regeneration.

In [emim]OAc, the high 9 w/w % pulp loading produced firm semiclear gels if water content was 16 w/w % (2.0 nH_2O/nIL) or above, but the mix remained clear (Supporting Information, Figure S3). At 22 w/w %, that is, at 1:2.66 stoichiometry, turbidity sharply jumped to a plateau, where further addition of water did not change the turbidity substantially, as described by Mazza et al. for [bmim]Cl.[29] The high scatter is a result of the high viscosity of the 9 w/w % mix, which makes removal of air bubbles more difficult.

The 1 w/w % solution of pulp in [emim]OAc was easier to handle, although centrifugation was necessary above 23 w/w % water content to remove air bubbles. The start of regeneration occurred at 18.32 w/w % and ended at 23.08 w/w % for [emim]OAc, which is similar but not exactly the same as in the 9 w/w % case. However, from the 1 w/w % data, the most remarkable result can be seen by plotting turbidity against stoichiometry of water per ionic liquid. The starts of regeneration are rather high and approximately similar, with stoichiometry of water n_{H_2O}/n_{IL} = 2.2−4.4, 3.1−5.6, and 2.1−2.8 for [TMGH]$EtCO_2$, [TMGH]OAc, and [emim]OAc, respectively (Figure 3), and additionally 2.5−3.0 for NMMO. Earlier, in the case of solutions in NMMO, such ranges instead of sharp thresholds have been explained by the polydispersity of the molecular weight distribution of cellulose.[41] Our data

dx.doi.org/10.1021/bm300912y | Biomacromolecules 2012, 13, 2896−2905

suggests that the width of the ranges is also dependent on the solvent.

In the case of [TMGH]OAc, the high threshold of regeneration aroused suspicions of side reactions. To check against acylation or carbamylation, the sample was washed to remove the IL. After washing with water four times and twice with ethanol, the infrared spectrum was identical to that of original pulp (see Supporting Information, Figure S4).

Rheology. The visco-elasticity of the samples changed noticeably upon addition of water (gel formation) without necessarily leading to a nephelometry signal. Thus, the visco-elastic properties were assessed by rheometry. For the 1 w/w % pulp-[emim]OAc solution, both oscillatory and steady shear tests were performed at 25 °C. To compare samples with varying water content, the dynamic parameter, that is, complex viscosity η^*, storage modulus G', and loss modulus G'', were captured at an angular velocity of 7.28 s^{-1}. At low water content, the mixtures did not differ significantly in terms of their viscoelastic properties. However, exceeding a threshold of 1.30 n_{H_2O}/n_{IL} (12 w/w %) all aforementioned dynamic parameters showed a steep rise until they reached a maximum at around 2.54 n_{H_2O}/n_{IL} (21 w/w %), which coincides approximately with the inflection point of the turbidity curve (Figure 3, Supporting Information, Figure S5). This indicates the complexity of the regeneration process in which the ultimate collapse of the gel-like transition phase and concomitant particle formation represents only one of four stages (see Discussion). Gel formation as the initial phase of regeneration was confirmed by steady shear measurements. At low water content, the (dynamic) viscosity curves show a Newtonian behavior over a wide shear range and shear thinning at high shear rates. However, as the relative amount of water exceeds 1.30 n_{H_2O}/n_{IL} (12 w/w %), the cellulose molecules form a supramolecular structure, expressed in a power law dependency of the viscosity curves, that is, a straight line with a slope of −1 in a double logarithmic plot (see Supporting Information, Figure S6). This transition from liquid-like to solid-like behavior was also observed by Song et al. when they gradually increased the MCC concentration in [emim]OAc.[42] In combination with our results it can be concluded that the so-called critical gel point of cellulose in ILs is not only a function of the solute concentration but also depends on the (residual) water content.

For the respective [TMGH]OAc mixtures, assessment of the solution state turned out to be more complex as the gel melting point was near or even below room temperature. Thus, temperature differences affect the rheological parameter more significantly. A frequency sweep at 25 °C revealed a sudden rise of dynamic moduli and complex viscosity, respectively, at a water content of 3.11 n_{H_2O}/n_{IL} (24.2 w/w %), which, in contrast to [emim]OAc, almost coincides with the onset of turbidity (Supporting Information, Figure S5). Although maintaining the exact same thermal history was not possible with this method, the samples were always handled below the gel melting point in turbidity experiments. To evaluate the effect of temperature, the [TMGH]OAc mixtures were subjected to a dynamic temperature sweep (heating/cooling cycle) at constant strain and angular velocity. The crossover of the dynamic moduli G' and G'' was then defined as sol−gel transition temperature (Supporting Information, Figure S7). All samples below a water content of 2.61 n_{H_2O}/n_{IL} (21.1 w/w %) remained viscous solutions within the tested temperature range of 20−100 °C. Starting from 2.61 n_{H_2O}/n_{IL}, the samples exhibited a linear relationship between water content and transition temperature (Supporting Information, Figure S8). Once liquefied, the initial network structure was not re-established instantaneously upon cooling. Instead, the mixtures entered a supercooled state. The resulting hysteresis is in accordance with previous studies.[42] Above 4.01 n_{H_2O}/n_{IL} (29.2 w/w %), the cellulose−IL−water mixtures formed a strong gel structure that did not melt within the tested range (up to 100 °C).

DISCUSSION

Regeneration. This study mainly focused on the regeneration of cellulose, that is cellulose was precipitated from a solution by adding water. Aside from the need to characterize the regeneration process when aiming for cellulosic products, this was also to avoid the influence of topochemical and fiber-specific diffusion effects that have to be taken into account when dissolving pulp in ILs with different water contents.[23,43]

The regeneration of a 1 w/w % cellulose solution in [emim]OAc and [TMGH]OAc was studied in detail by means of nephelometric, rheometric, and spectroscopic methods. Thereby, four stages leading to regenerated cellulose could be identified. First, the gradual addition of water to the IL-cellulose solutions causes an increase of the samples' storage modulus G' at 1.6 n_{H_2O}/n_{IL} for [emim]OAc and at 3.03 n_{H_2O}/n_{IL} for [TMGH]OAc, indicating the formation of a gel-like, supramolecular structure before turbidity is observed (Figure 3). This can be assigned to the hydrophobic interactions of cellulose, which is amphiphilic in that it has both hydrophilic hydroxyl groups and nonhydrophilic surfaces.[44,45] (This has recently been termed the Lindmann concept,[46] although numerous publications have addressed the amphiphilic character of cellulose already earlier.[47]) Computational studies have shown that the IL-cation can form van der Waals bonds to the nonhydrophobic C−H moieties of the anhydroglucose repeating unit and, thus, break the intersheet bonds of the supermolecular cellulose structure.[48−50] Conversely, these bonds are reformed first upon addition of water, as the hydration of the cation increases its steric demand and prohibits short-range dispersive interactions. At this stage, the cellulose interactions are still weak, reflected by the possible liquefaction of the gel upon heating, that is, the weak bonds can be broken and the gel turned into a visco-elastic fluid via heating the mixture beyond the sol−gel transition temperature (see Supporting Information, Figure S8 for [TMGH]OAc).[42]

The evolution of turbidity marks the beginning of the second regeneration phase. The water content thresholds of the studied IL−cellulose systems at which the turbidity signal starts to rise are given in Table 2. At this point, the liquid phase is in fact mostly water in stoichiometric terms, and the structure of the bulk solution is entirely disturbed. Since the cellulose hydroxyl-acetate bond is stronger than that to water,[25] the ILs will remain on the surface of the cellulose molecule, unless forcibly disturbed from the bulk. This is exacerbated by the fact that packing of a hydrophobic cation around the first anion solvation shell offers a barrier to the transport of water to the anion-cellulose H-bond. If the packing is tight, one would expect the bulky $[TMGH]^+$ cation to provide a suitable barrier to removal of IL from the solvation shell.

Table 1. List of Ionic Liquids Considered for Net Basicity

ionic liquid	π^*	α	β	$\beta-\alpha$	C[a]	KT	ionic liquid	π^*	α	β	$\beta-\alpha$	C[a]	KT
[TMGH]$EtCO_2$	0.990	0.704	1.164	0.460	x[27]	this	[bmim]HCOO	1.03	0.56	1.01	0.45	x[59]	59
[TMGH]OAc	1.041	0.530	1.095	0.565	x[27]	this	[bmim]EtCOO	0.96	0.57	1.10	0.53	x[59]	59
[emim]OAc	1.008	0.493	1.094	0.601	x[62]	16	[bmim]PrCOO	0.94	0.56	1.10	0.54	x[59]	59
NMMO·H_2O	1.067	0.205	0.969	0.763	x[2]	this	[bmim] t-BuCOO	0.91	0.54	1.19	0.65	x[59]	59
[emim] (MeO)$MePO_2$	1.06	0.50	1.07	0.57	x[19]	63	[bmim]$N(CN)_2$	1.129	0.464	0.708	0.244	o[21]	64
[emim] $(MeO)_2PO_2$	1.00	0.51	1.00	0.49	x[19]	19	[bmim]$MeOSO_3$	1.046	0.545	0.672	0.127	o[59]	21
[emim]NO_3	1.13	0.48	0.66	0.18		40	[bmim]TfO	0.974	0.643	0.483	−0.16	o[21]	21
[emim]ClO_4	1.11	0.56	0.41	−0.15		40	[bmim]BF_4	0.984	0.665	0.451	−0.214	o[58]	64
[emim]Tf_2N	0.99	0.76	0.28	−0.48	o[65]	40	[bmim]Tf_2N	0.971	0.635	0.248	−0.387	o[66]	64
[emim]PF_6	0.99	0.66	0.2	−0.46		40	[bmim]PF_6	1.032	0.634	0.207	−0.427	o[58]	67
[emim]$MeOSO_3$	1.09	0.57	0.61	0.04	o[68]	68	[P_{8888}]$MeHPO_3$	0.84	0.25	1.4	1.15	o[56]	56
[(HOC_2)mim] NO_3	1.11	0.77	0.65	−0.12		40	[P_{6666}]$MeHPO_3$	0.84	0.25	1.33	1.08	o[56]	56
[(HOC_2)mim] $N(CN)_2$		0.8	0.51	−0.29		40	[P_{4444}]$MeHPO_3$	0.84	0.25	1.28	1.03	o[56]	56
[(HOC_2)mim] Tf_2N	1.03	1.17	0.34	−0.83		40	[emim] $(MeO)HPO_2$	1.06	0.52	1.00	0.48	x[19]	57
[(HOC_2)mim] ClO_4	1.13	1.06	0.16	−0.9		40	[mmim] $(MeO)HPO_2$	1.08	0.53	0.99	0.46	x[57]	57
[(HOC_2)mim] OAc	1.04	0.53	0.9	0.37		40	[pmim] $(MeO)HPO_2$	1.02	0.54	1.00	0.46	x[57]	57
[(HOC_2)mim]Cl	1.16	0.73	0.68	−0.05		40	[bmim] $(MeO)HPO_2$	1.01	0.52	1.02	0.5	x[57]	57
[(HOC_2)mim] PF_6	1.11	1.17	0.15	−1.02		40	[amim] $(MeO)HPO_2$	1.06	0.51	0.99	0.48	x[57]	57
[HOC_2mim] $(MeO)HPO_2$	1.06	0.63	0.91	0.28	b[57]	57	[$MeOC_2$mim] $(MeO)HPO_2$	1.07	0.51	0.98	0.47	x[57]	57
[bmim]OAc	0.971	0.47	1.201	0.731	x[62]	21	[edmim] $(MeO)HPO_2$	1.11	0.33	1.01	0.68	b[57]	57
[bmim] $(MeO)_2PO_2$	0.97	0.452	1.118	0.666	x[21]	21	[empip] $(MeO)HPO_2$	1.08	0.29	1.08	0.79	b[57]	57
[bmim]Cl	1.03	0.49	0.83	0.34	x[58]	21	[N_{1222}] $(MeO)HPO_2$	1.14	0.29	1.04	0.75	b[57]	57

[a] x: good cellulose solvent; b: low solubility; o: explicitly confirmed nonsolvent.

dx.doi.org/10.1021/bm300912y | *Biomacromolecules* 2012, 13, 2896−2905

In the third stage, the phases separate, but the cellulose-bearing solid phase is perturbed by a water−IL mixture. The fourth stage comprises therefore the removal of the water−IL mixture from the regenerated cellulose-bearing gel. Thorough washing is required to force this to completion (see Supporting Information, Figures S4 and S9).

Net Basicity. There have been several previous attempts to correlate the swelling or dissolution of biomass with solvent parameters. As mentioned in the introduction, the polar (δ_P) and hydrogen bonding (δ_H) components of the Hildebrand parameter (δ) are correlated with swelling of cellulose in molecular solvents.[23] The swelling of pine wood chips in ILs has been correlated to the KT β value.[51] This is in line with our experiments which show that mainly the change of β upon addition of water correlates with cellulose regeneration. Reichardt's $E_T(30)$ value, which is solely a function of Reichardt's dye solvochromic response, was rather high for all liquids measured (49−52) and remained so upon the addition of water. For the $[TMGH]^+$ ILs, immediately upon addition of even 1 w/w % water, the value jumped by 1.7−2.9 units (Figure 2). However, this occurs below concentrations that precipitate cellulose (Figure 3). This effect is known for mixtures of water with molecular solvents[52] and has also been observed by Doherty et al. for α when adding water to [emim]OAc (see Figure 2c).[16] The decrease of the β value and the increase of the acidity of the mixture, particularly at low water contents, are best explained by the preferential solvation of water by the anion of the IL. Water has a low hydrogen bond basicity, but a high hydrogen bond acidity (β = 0.18, α = 1.17),[13] thus, it interacts with the anion. Moreover, ILs are known to increase the autoprotolysis (K_w) of water,[51] therefore, the acidity is expected to increase especially on addition of small amounts of water in an IL-dependent manner.

Although the change of β is the most significant one, it is doubtfully the only one relevant for cellulose solubility. Computational studies have already shown that also the cation has a role in the dissolution process.[48−50] When looking at other solution systems, the interactions of solvents and catalysts are described by the difference δ between the donor number (DN) and acceptor number (AN), two other solvatochromic parameters for quantifying hydrogen bonding acidity and basicity.[53] Consequently, a combined parameter, $\beta-\alpha$, was considered herein. To start with, our results were combined with available literature data of neat ILs (Table 1) and the "net basicity" ($\beta-\alpha$) of each IL was plotted versus its β value (Figure 4). In contrast to molecular solvents (see Supporting Information, Figure S10), the ($\beta-\alpha$) versus β plot for ILs shows a distinct correlation, indicating a strong dependency between α and β. A deviation is observed for the ILs bearing a hydroxyl group (1-(2-hydroxyethyl)-3-methylimidazolium [HOC_2mim]), which allows for stronger interion hydrogen bonding. Figure 4 reveals that all ILs reported to dissolve cellulose are located within a certain section. This allows the definition of an empirical "dissolution window": the β value ranges from 0.80 to 1.20, whereas the net basicity should neither be lower than 0.35 nor exceed 0.90, reflecting a necessary balance between acidity and basicity. The lower threshold value for β is in accordance with observations of Sellin et al.[54] and Gericke et al.[55] However, the limits of the dissolution window are diffuse to at least some extent, as depicted in Figure 4. Especially the upper limits are currently defined by one type of phosphonium-based ILs only ([P_{8888}]-$MeHPO_3$ has π^* = 0.84, α = 0.25, β = 1.40).[56] Nevertheless,

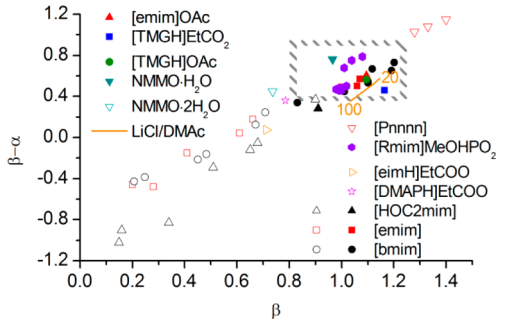

Figure 4. Difference $\beta-\alpha$ plotted against β, with the solvent window $0.35 < \beta-\alpha < 0.9$; full symbols are cellulose solvents, empty symbols nonsolvents. The left legend shows the solvents presented in this work. LiCl/DMAc data is shown in the range 20−100 °C. The right legend indicates the cations of various ILs reported in literature (the respective anions are listed in Table 1).

the net basicity plot allows to define cellulose solvent requirements more accurately than a simple α versus β plot (see Supporting Information, Figure S11).

As for molecular solvents, several seem to fit into the β range for dissolution, but there are none which have both a high π^* and $\beta-\alpha$ (see Supporting Information, Figure S10). The only $\beta-\alpha$ outlier in Figure 4 is [HOC_2mim](MeO)HPO_2, which dissolves only up to 6 w/w % cellulose when heated to 100 °C;[57] its hydroxyl group causes IL self-association. [bmim]Cl, which straddles the boundary at $\beta-\alpha$ = 0.34[58] (0.40 from another source[59]), also requires heating to 100 °C for a 10 w/w % solubility.

In addition, Figure 4 includes the known cellulose solvent system 6 w/w-% LiCl/DMAc which starts to drift out from the solvent range upon heating from 20 to 100 °C. Indeed, pulps do not defibrillate sufficiently to dissolve in hot LiCl/DMAc, but require impregnation with DMAc at 150 °C followed by addition of LiCl and cooling; the crystallinity index starts decreasing only at 80 °C.[9,10,60,61]

Correlation of Solvent Parameter and Regeneration. As mentioned in the Results section, the β value changes most significantly among all KT parameters upon water addition and, thus, seems likely to correlate with the cellulose precipitation (Figure 2). Figure 5 shows the $\beta-\alpha$ versus β plot for various IL−water mixtures. All of the ILs rapidly drift out from the net basicity solution window when adding water. However, water affects the liquids differently. [emim]OAc remains in the

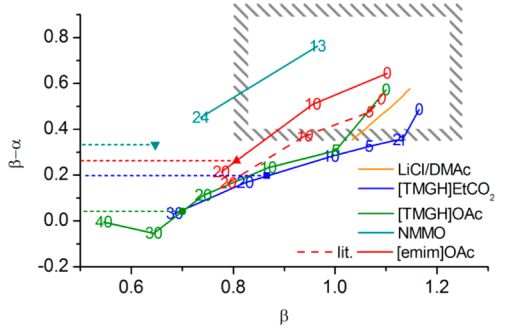

Figure 5. Effect of addition of water on basicity and net basicity; labels are water contents (w/w %) and symbols with drop lines are thresholds of regeneration; the rectangle depicted is the same as in Figure 4; values from Doherty et al.[16] are included.

dx.doi.org/10.1021/bm300912y | Biomacromolecules 2012, 13, 2896−2905

solvent window until a high water content (ca. 1.76 n_{H_2O}/n_{IL} or 16 w/w %), which is in accordance with the known high water tolerance of [emim]OAc in the course of cellulose dissolution. On the other hand, [TMGH]$EtCO_2$ exits the solvent window almost immediately on addition of even 1 w/w % (0.11 n_{H_2O}/n_{IL}) of water; accordingly, almost no water is tolerated in cellulose dissolution. The same applies to [TMGH]OAc, which requires about 4 w/w % or 0.43 n_{H_2O}/n_{IL}. NMMO is a very good fit to the $\beta-\alpha$ minimum of the solvent window, whereas if β only is considered, turbidity appears at comparatively low β.

The KT values at which regeneration can be observed are highlighted in Figure 5 and summarized in Table 2. They are slightly outside the dissolution window which was developed with solubility data of neat ILs. This highlights again the distinct difference between dissolution and regeneration of cellulose in ILs. It has to be noted that the regeneration thresholds are not exact values because of kinetically hampered regeneration, that is, the system can remain in a solution state even though the critical water threshold has been passed and then forms gradually a gel or a suspension in the course of hours or even days (cf. retrogradation of starch).[17]

Table 2. Kamlet–Taft Parameters of Pure IL–Water Mixtures at Water Contents Where the Respective 1 w/w % Cellulose Solution Start to Regenerate (Identified via Onset of Turbidity, cf. Figure 3)

solvent	w/w %[a]	n/n[b]	π^*	α	β	$\beta-\alpha$
[TMGH]$EtCO_2$	17	2.22	1.00	0.67	0.87	0.20
[TMGH]OAc	24	3.11	1.14	0.66	0.70	0.04
[emim]OAc	18	2.12	1.05	0.54	0.81	0.26
NMMO·nH_2O	28	2.47	1.09	0.32	0.65	0.33

[a]Weight % of water in IL. [b]Stoichiometry of water per IL.

Differences between the Cellulose Solvents. To explain the differing behavior of the IL solvents upon regeneration, the strong H-bonding interactions between the solvents and cellulose are relevant. In the bulk, the $[TMGH]^+$ cation functions as a hydrotrope, decreasing water availability at lower concentrations; thus, the cellulose solutions in [TMGH]-based ILs regenerate at higher water contents than those of [emim]OAc. However, the $[TMGH]^+$ cation is bulky due to its dimethylamine groups, which will create a more impervious hydrophobic surface on the solvated complex, making it less susceptible to intrusion from water. In addition to this, due to the increased acidity of the $[TMGH]^+$ versus the $[emim]^+$ cations, the interaction between the ion pairs is stronger for the [TMGH]-based ILs and their associated complexes. This likely strengthens the resistance of the cellulose-IL complex toward attack from water during regeneration. For [emim]OAc, the anion–cation H-bonding interaction is weaker, allowing for more mobility of the ions. In addition, the cation is more electronically diffuse, less sterically hindered and, therefore, more susceptible to dissolution with water. In the variation of the anion, the extra methylene in propionate versus acetate likely causes more steric crowding, reducing the stability of the solvated complex. Thus, the order of water tolerance of predissolved cellulose solutions is observed to be [TMGH]OAc < [TMGH]$EtCO_2$ ≪ [emim]OAc. NMMO–water retains a high β throughout the regeneration (Figure 5); cellulose precipitates exactly at the predicted $\beta-\alpha$ boundary ($\beta-\alpha$ = 0.33), while β goes as low as 0.65 (Table 2). This again shows that value of $\beta-\alpha$ is a more general descriptor for regeneration than β alone. Apparently, NMMO precipitates cellulose much more cleanly upon addition of water, thus, the match to the predicted $\beta-\alpha$ is better than for ILs, whereas the ILs are more easily retained on the cellulose.

In contrast, dissolution, which includes a decrystallization transition, is different from regeneration. The inability to dissolve cellulose in wet [TMGH] ILs can be explained as an effect of the increased acidity of water in these ILs, which push these ILs out of the solvent range, as detailed in Figure 5. This effect is weaker for [emim]OAc, which is a weaker autoprotolysis enhancer, demonstrated by the sudden increase of α at low water contents (Figure 2). This allows even wet [emim]OAc solutions (10–15 w/w % H_2O) to dissolve cellulose. One would rationally expect that a higher β basicity of [emim]OAc would explain this, but the β values are similar at low water contents.

Conclusions. The aim of this study was to correlate Kamlet–Taft solubility parameter of ionic liquids with their capability to dissolve and regenerate cellulose. α, β, π^*, and $E_T(30)$ of [emim]OAc, [TMGH]OAc, and [TMGH]$EtCO_2$ were determined as a function of water content and temperature. In addition, the known cellulose solvents NMMO·H_2O and LiCl/DMAc were studied as well. As expected, it was found that the KT β values decrease significantly with the addition of water. The π^* value increased, and α and $E_T(30)$ remained approximately constant after a small initial jump at 1 w/w % water or below. KT values other than β were not found to correlate directly with dissolution of cellulose. Among the single KT parameters, the β value is that which explains dissolution best. However, the match was inexact for regeneration with water (Table 2). Consequently, the net basicity $\beta-\alpha$ was considered instead for both dissolution and regeneration, which better accounts for the acidity imparted by the cation, or protic cosolvent, particularly for NMMO·H_2O. KT values of neat ILs from literature were added to create $\beta-\alpha$ versus β plot. In this plot, the cellulose dissolving ILs could be located in a region roughly defined by $0.35 < \beta-\alpha < 0.9$ and $0.80 < \beta < 1.20$. The regeneration of cellulose could be divided into four stages: gelation, particle formation, regenerated cellulose with IL/water adsorbed, removal of residual IL via excessive washing. The distinct difference between dissolution and regeneration is clearly demonstrated by [TMGH]OAc and [TMGH]$EtCO_2$. Although they are very sensitive toward water when dissolving cellulose, they tolerate more water when regenerating the cellulose from solution. Due to the hydrotropic nature of the more bulky cations, cellulose regeneration may require more hydrophobic mixtures (e.g., water–alcohols) for more efficient regeneration of pure cellulose.

The solubility window in combination with an understanding of the regeneration of cellulose from the respective solutions could help to seek more efficiently for new cellulose dissolving ILs as it stresses the importance of α in both dissolution and regeneration.

■ ASSOCIATED CONTENT

Supporting Information

Water content determination and IR details; equations used to calculate KT parameter; for each dye and temperature, thermochromicity represented as linear functions of wavelength per temperature; nephelometry results of 9 w/w % pulp in [emim]OAc; graphs for noncorrelated variable pairs ($\beta-\alpha$, β)

for molecular solvents and (β, α) for ILs; ATR-IR spectra of each washing step in washing [TMGH]OAc 1 w/w-% cellulose solution with water; steady shear viscosity of 1 w/w % pulp in [emim]OAc with different water contents; comparison of [emim]OAc and [TMGH]OAc with respect to turbidity and storage modulus; for [TMGH]OAc 1 w/w % cellulose solution, a frequency sweep at 25 °C, a temperature ramp 20−100 °C and a graph of sol−gel transition point and dynamic moduli versus water content; a schematic of the regeneration process; a photograph of wet [TMGH]OAc mixed with pulp. This material is available free of charge via the Internet at http://pubs.acs.org.

AUTHOR INFORMATION

Corresponding Author

*Tel.: +358 (0)9 4702 4201. E-mail: herbert.sixta@aalto.fi.

Notes

The authors declare no competing financial interest.

ACKNOWLEDGMENTS

This work was financed by Forestcluster Ltd. and Tekes in the framework of the Future Biorefinery project.

REFERENCES

(1) Liebert, T. In *Cellulose Solvents: For Analysis, Shaping and Chemical Modification*; ACS Symposium Series; American Chemical Society: Washington, DC, 2010; Vol. *1033*, pp 3−54.

(2) Johnson, D. L. U.S. Patent 3,508,941, 1970.

(3) Fink, H. P.; Weigel, P.; Purz, H. J.; Ganster, J. *Prog. Polym. Sci.* **2001**, *26*, 1473−1524.

(4) Rosenau, T.; Potthast, A.; Sixta, H.; Kosma, P. *Prog. Polym. Sci.* **2001**, *26*, 1763−1837.

(5) Lindman, B.; Karlström, G.; Stigsson, L. *J. Mol. Liq.* **2010**, *156*, 76−81.

(6) Taylor, J. B. *Trans. Faraday Soc.* **1957**, 1198−1203.

(7) Kamida, K.; Okajima, K.; Matsui, T.; Kowsaka, K. *Polym. J.* **1984**, *12*, 857−866.

(8) Graenacher, C. U.S. Patent 1,943,176, 1934.

(9) McCormick, C. L. U.S. Patent 4,278,790, 1981.

(10) McCormick, C. L.; Callais, P. A.; Hutchinson, B. H. *Macromolecules* **1985**, *12*, 2394−2401.

(11) Remsing, R. C.; Swatloski, R. P.; Rogers, R. D.; Moyna, G. *Chem. Commun.* **2006**, *12*, 1271−1273.

(12) Spange, S.; Reuter, A.; Vilsmeier, E.; Heinze, T.; Keutel, D.; Linert, W. *J. Polym. Sci., Part A: Polym. Chem.* **1998**, *11*, 1945−1955.

(13) Kamlet, M. J.; Abboud, J. L. M.; Abraham, M. H.; Taft, R. W. *J. Org. Chem.* **1983**, *17*, 2877−2887.

(14) Dimroth, K.; Reichardt, C.; Siepmann, T.; Bohlmann, F. *Liebigs Ann.* **1963**, *1*, 1−37.

(15) Reichardt, C. *Solvents and Solvent Effects in Organic Chemistry*; Wiley-VCH: Weinheim, 2003; pp 629−416.

(16) Doherty, T. V.; Mora-Pale, M.; Foley, S. E.; Linhardt, R. J.; Dordick, J. S. *Green Chem.* **2010**, *11*, 1967−1975.

(17) Eliasson, A.-E. Gelatinization and retrogradation of starch in foods and its implications for food quality. In *Chemical Deterioration and Physical Instability of Food and Beverages*; Skibsted, L. H., Risbo, J., Andersen, M. L., Eds.; Woodhead Publishing Limited: Oxford, U.K., 2010; pp 296−323.

(18) Rinaldi, R. *Chem. Commun.* **2011**, *1*, 511−513.

(19) Fukaya, Y.; Hayashi, K.; Wada, M.; Ohno, H. *Green Chem.* **2008**, *1*, 44−46.

(20) Fukaya, Y.; Sugimoto, A.; Ohno, H. *Biomacromolecules* **2006**, *12*, 3295−3297.

(21) Brandt, A.; Hallett, J. P.; Leak, D. J.; Murphy, R. J.; Welton, T. *Green Chem.* **2010**, *4*, 672−679.

(22) Krässig, H. A. *Cellulose: Structure, Accessibility and Reactivity*; Gordon and Breach Science Publishers: Chemin de la Sallaz, Switzerland, 1993; Vol. *11*, pp 376.

(23) Philipp, B.; Schleicher, H.; Wagenknecht, W. In *The Influence of Cellulose Structure on the Swelling of Cellulose in Organic Liquids*; International Symposium on Macromolecules; Harva, O., Overberger, C. G., Eds.;John Wiley & Sons: New York, NY, 1973; Vol. *43*, pp 1531−1543.

(24) El Seoud, O.; Fidale, L.; Ruiz, N.; D'Almeida, M.; Frollini, E. *Cellulose* **2008**, *3*, 371−392.

(25) Liu, H.; Sale, K. L.; Holmes, B. M.; Simmons, B. A.; Singh, S. *J. Phys. Chem. B* **2010**, *12*, 4293−4301.

(26) Kahlen, J.; Masuch, K.; Leonhard, K. *Green Chem.* **2010**, *12*, 2172−2181.

(27) King, A. W. T.; Asikkala, J.; Mutikainen, I.; Järvi, P.; Kilpeläinen, I. *Angew. Chem.* **2011**, *28*, 6425−6429.

(28) Wilkes, J. S.; Zaworotko, M. J. *J. Chem. Soc., Chem. Commun.* **1992**, *13*, 965−967.

(29) Mazza, M.; Catana, D.; Vaca-Garcia, C.; Cecutti, C. *Cellulose* **2009**, *16*, 207−215.

(30) VanRheenen, V.; Cha, D. Y.; Hartley, W. M. *Org. Syn.* **1978**, *58*, 43.

(31) Bevilaqua, T.; da Silva, D. C.; Machado, V. G. *Spectrochim. Acta, Part A* **2004**, *4*, 951−958.

(32) Silva, M. A. d. R.; da Silva, D. C.; Machado, V. G.; Longhinotti, E.; Frescura, V. L. A. *J Phys. Chem. A* **2002**, *37*, 8820−8826.

(33) Kosan, B.; Michels, C.; Meister, F. *Cellulose* **2008**, *1*, 59−66.

(34) Gericke, M.; Schlufter, K.; Liebert, T.; Heinze, T.; Budtova, T. *Biomacromolecules* **2009**, *5*, 1188−1194.

(35) Sammons, R. J.; Collier, J. R.; Rials, T. G.; Petrovan, S. *J. Appl. Polym. Sci.* **2008**, *2*, 1175−1181.

(36) Biganska, O.; Navard, P. *Polymer* **2003**, *4*, 1035−1039.

(37) Stenutz, R. Tables for Chemistry - Kamlet-Taft solvent parameters. http://www.stenutz.eu/chem/solv26.php (accessed 08/23/2011).

(38) Tada, E. B.; Novaki, L. P.; El Seoud, O. A. *J. Phys. Org. Chem.* **2000**, *13*, 679−687.

(39) Angyal, S. J.; Warburton, W. K. *J. Chem. Soc.* **1951**, 2492−2494.

(40) Zhang, S.; Qi, X.; Ma, X.; Lu, L.; Deng, Y. *J. Phys. Chem. B* **2010**, *11*, 3912−3920.

(41) Eckelt, J.; Eich, T.; Röder, T.; Rüf, H.; Sixta, H.; Wolf, B. *Cellulose* **2009**, *3*, 373−379.

(42) Song, H.; Niu, Y.; Wang, Z.; Zhang, J. *Biomacromolecules* **2011**, *4*, 1087−1096.

(43) Cuissinat, C.; Navard, P.; Heinze, T. *Carbohydr. Polym.* **2008**, *4*, 590−596.

(44) Biermann, O.; Hädicke, E.; Koltzenburg, S.; Müller-Plathe, F. *Angew. Chem., Int. Ed.* **2001**, *20*, 3822−3825.

(45) Lindman, B.; Karlström, G.; Stigsson, L. *J. Mol. Liq.* **2010**, *1*, 76−81.

(46) Medronho, B.; Romano, A.; Graça Miguel, M.; Stigsson, L.; Lindman, B. *Cellulose* **2012**, *19*, 581−587.

(47) Glasser, W. G.; Atalla, R. H.; Blackwell, J.; Brown, R. M., Jr.; Burchard, W.; French, A. D.; Klemm, D. O.; Navard, P.; Nishiyama, Y. *Cellulose* **2012**, *19*, 589−598.

(48) Liu, H.; Sale, K. L.; Simmons, B. A.; Singh, S. *J. Phys. Chem. B* **2011**, *34*, 10251−10258.

(49) Gross, A. S.; Chu, J.-W. *J. Phys. Chem. B* **2010**, *114*, 13333−13341.

(50) Min Cho, H.; Gross, A. S.; Chu, J.-W. *J. Am. Chem. Soc.* **2011**, *133*, 14033−14041.

(51) Zhang, Y.; Du, H.; Qian, X.; Chen, E. Y. X. *Energy Fuels* **2010**, *4*, 2410−2417.

(52) Cheong, W. J.; Carr, P. W. *Anal. Chem.* **1988**, *8*, 820.

(53) Takagi, H.; Isoda, T.; Kusakabe, K.; Morooka, S. *Energy Fuels* **1999**, *6*, 1191−1196.

(54) Sellin, M.; Ondruschka, B.; Stark, A in *Cellulose Solvents: For Analysis, Shaping and Chemical Modification*; ACS Symposium Series;

American Chemical Society: Washington, DC, 2010; Vol. *1033*, pp 121−135.
(55) Gericke, M.; Liebert, T.; El Seoud, O. A.; Heinze, T. *Macromol. Mater. Eng.* **2011**, *296*, 483−493.
(56) Ohno, H. *Polar Ionic Liquids for a Sustainable World*, Pacifichem 2010, International Chemical Congress of Pacific Basin Societies, Honolulu, Hawaii, USA, December 15-20, 2010; Canadian Society for Chemistry: Honolulu, Hawaii, USA, 2010.
(57) Fukaya, Y.; Hayashi, K.; Kim, S. S.; Ohno, H. Design of Polar Ionic Liquids To Solubilize Cellulose without Heating. In *Cellulose Solvents: For Analysis, Shaping and Chemical Modification*; ACS Symposium Series; American Chemical Society: Washington, DC, 2010; Vol. *1033*, pp 55−66.
(58) Swatloski, R. P.; Spear, S. K.; Holbrey, J. D.; Rogers, R. D. *J. Am. Chem. Soc.* **2002**, *18*, 4974−4975.
(59) Ohno, H.; Fukaya, Y. *Chem. Lett.* **2009**, *1*, 2−7.
(60) Turbak, A. F.; El-Kafrawy, A.; Snyder, F. W., Jr.; Auerbach, A. B. U.S. Patent 4,302,252, 1981.
(61) Ramos, L. A.; Assaf, J. M.; El Seoud, O. A.; Frollini, E. *Biomacromolecules* **2005**, *5*, 2638−2647.
(62) Stegmann, V.; Massonne, K.; Maase, M.; Uerdingen, E.; Lutz, M.; Hermanutz, F.; Gaehr, F. U.S. Patent Application 20080269477, 2008.
(63) Swiderski, K.; McLean, A.; Gordon, C. M.; Vaughan, D. H. *Chem. Commun.* **2004**, *19*, 2178−2179.
(64) Chiappe, C.; Pieraccini, D.; Zhao, D.; Fei, Z.; Dyson, P. *Adv. Synth. Catal.* **2006**, *1*−*2*, 68−74.
(65) Hauru, L. K. J.; Hummel, M.; Sixta, H. In *Fractionation of Birch, Spruce and Pine in 1-Ethyl-3-methylimidazolium Acetate*; 241th ACS National Meeting; American Chemical Society: Anaheim, CA, 2011; CELL-297.
(66) Lozano, P.; Bernal, B.; Bernal, J. M.; Pucheault, M.; Vaultier, M. *Green Chem.* **2011**, *6*, 1406−1410.
(67) Crowhurst, L.; Mawdsley, P. R.; Perez-Arlandis, J. M.; Salter, P. A.; Welton, T. *Phys. Chem. Chem. Phys.* **2003**, 2790−2794.
(68) Hayashi, K.; Fukaya, Y.; Ohno, H. In *Design of Ionic Liquids to Dissolve Cellulose Without Heating*; Extended Abstracts of COIL-2; 2nd International Congress on Ionic Liquids, Yokohama, Japan, 2007; Tokyo University of Agriculture and Technology: Yokohama, Japan, 2007; pp 1P03-045.